Performance of a Model for a Local Neuron Population

L. H. Zetterberg,[1] L. Kristiansson,[2] and K. Mossberg[1]

[1] Telecommunication Theory, Royal Institute of Technology, Stockholm, and
[2] Information Theory and Data Transmission, Chalmers Institute of Technology, Gothenburg, Sweden

Abstract. A model of a local neuron population is considered that contains three subsets of neurons, one main excitatory subset, an auxiliary excitatory subset and an inhibitory subset. They are connected in one positive and one negative feedback loop, each containing linear dynamic and nonlinear static elements. The network also allows for a positive linear feedback loop. The behaviour of this network is studied for sinusoidal and white noise inputs. First steady state conditions are investigated and with this as starting point the linearized network is defined and conditions for stability is discovered. With white noise as input the stable network produces rhythmic activity whose spectral properties are investigated for various input levels. With a mean input of a certain level the network becomes unstable and the characteristics of these limit cycles are investigated in terms of occurence and amplitude. An electronic model has been built to study more closely the waveforms under both stable and unstable conditions. It is shown to produce signals that resemble EEG background activity and certain types of paroxysmal activity, in particular spikes.

1. Introduction

During the last few years there has been a stimulating activity in developing new methods for the analysis of electroencephalograms by means of computers. Of special interest are those methods that are based on mathematical models of the EEG signals which often take the form of noise generators followed by fairly simple spectral forming linear filters. It has been proved that such models can generate signals that closely resemble normal background EEG activity (Zetterberg, 1973; Zetterberg and Ahlin, 1975; Isaksson and Wennberg, 1975). This is of fundamental importance for the analysis but it also raises the question whether it is possible formulate models based

on neurophysiological facts that describe the generation of EEG signals. If this is the case it may indicate how data processing of EEG signals should be further developed. It may lead to definition of appropriate information carrying parameters for normal background activity and it may allow the analysis to be extended to cover various forms of paroxysmal activity.

There are many verbal descriptions of the basic neuronal activity and its relation to the observed EEG signals of which we mention the following that have influenced our thinking, Stevens (1966), Andersen and Andersson (1968) and the survey edited by Creutzfeld (1974). It shows how rich and variable the observed phenomena are and how complex the relation is between activity on the cellular level and measured potential differences in the cortex. But it also makes clear the intimate relation between the slow postsynaptic potentials, PSP, and the EEG. It is interesting to notice that several attempts have been made to formalize these neurophysiological facts into mathematical models that describe the electrical activity within local populations of neurons such as Levy and Etevenon (1972) and Etevenon and Levy (1973). Our paper is directly based on such works carried out by Wilson and Cowan (1972) and by Freeman (1972). Both publications deal with the interaction within and between a set of excitatory and a set of inhibitory neurons. Wilson and Cowan (1973) extended their model to hold for a population of neurons distributed on a surface and hence allowed both temporal and spatial interaction to occur. Freeman (1975) has written an extensive survey on how neurons may interact in simple and complex configurations. Expressed in engineering terms the main interest of Freeman is the transfer function and the impulse response of the stable (linearized) system while Wilson and Cowan are interested in the response to constant or pulsed stimulus and to the occurence of instabilities or limit cycles.

Based on the paper by Wilson and Cowan (1972) a simple lumped circuit model was formulated that interconnected the excitatory and inhibitory subsets in a negative feedback loop. Each subset was described by a linear dynamic element, related to the postsynaptic potential, and a nonlinear static element relating the average membrane potential within the cell population to the pulse rate of action potentials (Zetterberg, 1973; Lopes da Silva et al., 1974). The analysis was carried out for a linearized approximation of the network in order to express the transfer function of the network and the power spectrum of the average membrane potential. Numerical data of the postsynaptic potentials were taken from measurements on cells in thalamus in which case the network produced rhythmic activity consistent with the alpha activity.

Later the analysis was extended to take into account a first approximation of the nonlinear behaviour (Lopes da Silva et al., 1976). In an attempt to simulate the hippocampal theta rhythm the same reference argued for the inclusion of also a positive feedback loop through a third set of neurons. Freeman (1975) also includes such loops for models of parts of the olfactory system.

We will reformulate our previous model starting from Wilson and Cowan (1972) but this time also take into account the presence of the neuronal refractory period. The basic model is extended to include both positive and negative feedback loops. A steady state analysis is carried out which is used to establish the operating conditions for the linearized network. It will make the transfer function depend on the input level and it will show for what values of input level and parameter values that the network is stable or unstable. Next the network is analyzed when it is unstable and the characteristics of these oscillations, limit cycles, are established. They also depend upon input level and network parameters.

An electronic realization of the network has been built and experiments were carried out for both sinusoidal and noise inputs with the network in stable or unstable conditions. We have been able to imitate both background EEG activity and certain types of paroxysmal activity. It is of special interest that we can establish the presence of spikes as a boarderline case between stability and instability.

2. Formulation of a Lumped Circuit Neuron Model

2.1. Basic Equations

A population of neurons will be considered that contains two subsets, an excitatory and an inhibitory subset. Later a third subset will be added. The population is well localized and each subset behaves homo-geneously and hence no spatial variables will be introduced. Following Wilson and Cowan (1972) the variables $E(t)$ and $I(t)$ are defined, which will measure respectively the proportion of excitatory and inhibitory cells firing per unit of time at time t. The action potentials will spread through axons and reach synaptic contacts where they will be transformed into synaptic potentials. These will propagate through the dendrites and reach other cells with a certain delay and attenuation. These potentials will sum linearly to form a cell membrane potential which may cause the cell to fire.

Essential variables are the average membrane potentials $V_e(t)$ and $V_i(t)$ in the excitatory and inhibitory cell populations respectively. The potentials may be expressed as follows

$$V_e(t) = \int_0^\infty [c_3' E(t-\tau) + P(t-\tau)] h_e(\tau) d\tau$$
$$- \int_0^\infty c_2' I(t-\tau) h_i(\tau) d\tau \qquad (2.1.1)$$

$$V_i(t) = \int_0^\infty [c_1' E(t-\tau) + Q(t-\tau)] h_e(\tau) d\tau$$
$$- \int_0^\infty c_4' I(t-\tau) h_i(\tau) d\tau \qquad (2.1.2)$$

The constants c_3' and c_2' may be interpreted as the average number of excitatory and inhibitory synapsis per excitatory cell and correspondingly c_1' and c_4' are defined for the inhibitory cell population. Hence $c_3' E(t)$ and $c_2' I(t)$ are the average number of synapsis of an excitatory cell that will receive an action potential from the population itself during one time unit and $P(t)$ should be interpreted as the average number of excitatory pulses from outside per cell and time unit. Correspondingly $Q(t)$ is defined. The functions $h_e(\tau)$ and $h_i(\tau)$ are essentially the excitatory and inhibitory postsynaptic potentials, EPSP and IPSP respectively, but they may also include attenuation and delay due to pulse transmission and passive spread of the postsynaptic potentials.

Expressions (2.1.1) and (2.1.2) are essentially the same as derived by Wilson and Cowan (1972) but $h_e(\tau)$ and $h_i(\tau)$ need not be identical. It is now assumed that the fraction $E(t)$ of excitatory cells that will fire during a time unit at time t will be proportional to the probability that the membrane potential of a cell is above a threshold and at the same time it is in an excitatory state, i.e. it should not be in its refractory period.

The probability that an excitatory cell is excitable may be written

$$1 - \int_{t-r_e}^t E(t') dt' \qquad (2.1.3)$$

with r_e the absolute refractory period. Assumptions made by Wilson and Cowan (1972) imply that the conditional probability that a cell will fire given that it is in an excitatory state only depends upon the average potential in the subset, i.e. upon $V_e(t)$ for the excitatory subset. As a result

$$E(t) = \lambda_e \left[1 - \int_{t-r_e}^{t} E(t')dt' \right] f(V_e(t)) \qquad (2.1.4)$$

and similarly for the inhibitory subset

$$I(t) = \lambda_i \left[1 - \int_{t-r_i}^{t} I(t')dt' \right] f(V_i(t)) \qquad (2.1.5)$$

The proportionality constants λ_e and λ_i measure the maximum average firing rate of a cell in the two subsets. At most λ_e and λ_i can be r_e^{-1} and r_i^{-1} respectively but likely they are less. The function $f(x)$ must be monotone and increasing from 0 to 1 as x increases from its lowest to its highest value. The curve is often assumed to have an S-shaped form and it is then said to be a sigmoid curve.

Now the refractory periods r_e and r_i are about 1–2 ms (Wilson and Cowan, 1972, 1973) which is short compared to the time constants of the entire network and hence to the period or correlation time of the processes we are primarily interested in. Hence it is reasonable to replace the integrals in (2.1.4) and (2.1.5) with the expressions $r_e E(t)$ and $r_i I(t)$ respectively. They may then be solved for $E(t)$ and $I(t)$

$$E(t) = \frac{\lambda_e f(V_e(t))}{1 + \lambda_e r_e f(V_e(t))} \equiv \lambda_e g_e(V_e(t)) \qquad (2.1.6)$$

$$I(t) = \frac{\lambda_i f(V_i(t))}{1 + \lambda_i r_i f(V_i(t))} \equiv \lambda_i g_i(V_i(t)) \qquad (2.1.7)$$

The new functions $g_e(x)$ and $g_i(x)$ also have a sigmoid shape but with less slope than $f(x)$. It is seen that $E(t)$ and $I(t)$ have their largest attainable values $\lambda_e(1 + \lambda_e r_e)^{-1}$ and $\lambda_i(1 + \lambda_i r_i)^{-1}$ respectively.

It is interesting to notice that the presence of a refractory period has been taken into account through a transformation of the nonlinear function from $f(x)$ into either $g_e(x)$ or $g_i(x)$.

2.2. Block Diagram Representation and Generalization

It is convenient to draw a functional block diagram of the basic Eqs. (2.1.1), (2.1.2), (2.1.6), and (2.1.7) as in Fig. 1a. It contains linear dynamic blocks (filters) whose impulse response $h_e(\tau)$ or $h_i(\tau)$ represent the postsynaptic potentials, EPSP and IPSP respectively. The cell somas of each neuron subpopulation is reproduced by a summation unit where the EPSP and IPSP are summed with positive and negative sign respectively.
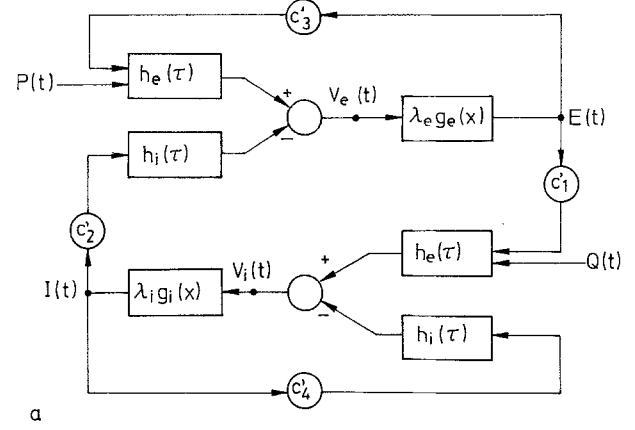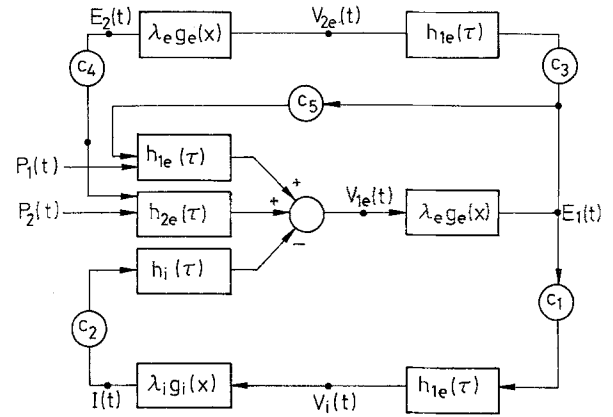
Fig. 1a and b. Block diagram of systems to model a local neuron population **a** system with one excitatory and one inhibitory subset of neurons, **b** system with two excitatory and one inhibitory subset of neurons

The nonlinear blocks marked $\lambda_e g_e(x)$ and $\lambda_i g_i(x)$ express the generation of action potentials while the outputs $E(t)$ and $I(t)$ denote the intensity of action potentials.

The two neuron populations are interconnected through c_2' and viewed from the excitatory subset it forms a negative feedback loop. The model includes also a linear feedback loop for each subset controlled through constants c_3' and c_4'. The neurophysiological counterpart is short connections (collaterals) from the axon to the soma for individual cells. Notice that the sign is preserved for the linear feedback loops.

The previously analyzed model (Lopes da Silva et al., 1972) excluded the linear feedback loops, i.e., c_3' and c_4' were put equal to zero and furthermore $\lambda_e g_e(x)$ and $\lambda_i g_i(x)$ were replaced by $f(x)$.

The model to be analyzed in this paper is shown in Fig. 1b. The main excitatory neurons interact with inhibitory interneurons giving negative feedback and with a third set of excitatory neurons giving positive feedback. It also allows for a linear positive feedback

loop through c_5 for the main excitatory subset to represent collateral connections. As can be seen from the figure two types of excitatory impulse responses $h_{1e}(\tau)$ and $h_{2e}(\tau)$ are introduced. They are distinguished through different delays with $h_{2e}(\tau)$ having the longer delay. Hence we may write

$$h_{2e}(\tau) = h_{1e}(\tau - \tau_d) \qquad (2.2.1)$$

Different inputs are being fed to the two impulse response blocks with $P_1(t)$ called specific input and $P_2(t)$ non-specific input using neurophysiological terminology.

The model in Fig. 1b was proposed to describe the behaviour of a local population in cortex in which case the main excitatory neurons were identified as pyramidal cells (meeting at the Neurophysiological Institute in Vienna). However, the model may also be seen as a fairly general network that covers several previously considered cases of neuronal models. It should therefore be of interest to study the behaviour of such a network.

The average membrane potential $V_{1e}(t)$ of the main excitatory cells may be thought of as the main output since it fairly closely follows the measured extracellular potential. The latter is essentially equal to $V_{1e}(t)$ with the DC component removed. The variables $E_1(t)$, $E_2(t)$, and $I(t)$ also have interest as indicators of the network and its behaviour.

2.3. Specific Assumptions

Wilson and Cowan (1972, 1973) use the simplest possible expression for the EPSP and IPSP, namely

$$h(\tau) = A \exp\{-a\tau\} ; \qquad \tau \geq 0 \qquad (2.3.1)$$

with $h(\tau) = 0$ for $\tau < 0$. The next level of sophistication is the following expression which takes better account of the interaction within the subpopulation (Zetterberg, 1973; Freeman, 1975).

$$h(\tau) = A[\exp\{-a\tau\} - \exp\{-b\tau\}] \qquad (2.3.2)$$

with $b > a$. In both cases the wave form has a steep increase and a slow decay. Only the last form will be used in the numerical analysis for which the following parameters are chosen, see also Lopes da Silva et al. (1974, 1976).

Excitatory subset:
$a_e = 55\,\mathrm{s}^{-1}$
$b_e = 605\,\mathrm{s}^{-1}$
$A = 1.6\,\mathrm{mV}$

Inhibitory subset:
$a_i = 27.5\,\mathrm{s}^{-1}$
$b_i = 55\,\mathrm{s}^{-1}$
$A = 32\,mV$

For later reference it is convenient to have an expression for the Laplace transform of (2.3.2) available,

also called the transfer function of the PSP network

$$H(s) = \frac{(b-a)A}{(s+a)(s+b)}. \qquad (2.3.3)$$

In this way $H_{1e}(s)$, $H_{2e}(s)$, and $H_i(s)$ are defined with

$$H_{2e}(s) = H_{1e}(s)\exp\{-s\tau_d\}. \qquad (2.3.4)$$

Various hypotheses have been put forward concerning the non-linear function $f(x)$ introduced in Sect. 2.1. Freeman (1975) argues for the following form

$$f(v) = \begin{cases} f_0 \exp\{2\gamma'(v-v_0)\} ; & v \leq v_0 \\ f_0[3 - 2\exp\{-\gamma'(v-v_0)\}] ; & v > v_0 \end{cases} \qquad (2.3.5)$$

with $\gamma' = 0.25$ to $2.0\,(\mathrm{mV})^{-1}$. Based on this assumption $g(v)$ has been calculated according to (2.1.6) and (2.1.7) with $\lambda_e r_e = \lambda_i r_i = 0.75$. As a reasonable compromise the following function $g(v)$ is chosen for both $g_e(v)$ and $g_i(v)$.

$$g(v) = \begin{cases} g_0 \exp\{\gamma(v-v_0)\} ; & v \leq v_0 \\ g_0[2 - \exp\{-\gamma(v-v_0)\}] ; & v > v_0 \end{cases} \qquad (2.3.6)$$

with $\gamma = 0.34\,(\mathrm{mV})^{-1}$. In the following numerical calculations $v_0 = 6\,\mathrm{mV}$ and $2g_0\lambda_e = 2g_0\lambda_i = 50\,\mathrm{s}^{-1}$ are being used.

3. Linear Analysis

3.1. Steady State Analysis

For the linear analysis it is assumed that the input signals $P_1(t)$ and $P_2(t)$ present only small variations around the steady state values $\bar{P}_1$ and $\bar{P}_2$. As a result the membrane potentials $V_{1e}(t)$, $V_{2e}(t)$, and $V_i(t)$ introduced in Fig. 1b will also show only small variations around their steady state values $\bar{V}_{1e}$, $\bar{V}_{2e}$, and $\bar{V}_i$. The same applies to the related variables $E_1(t)$, $E_2(t)$, and $I(t)$ with their steady state values denoted $\bar{E}_1$, $\bar{E}_2$, and $\bar{I}$.

With inputs $P_1(t) = \bar{P}_1$ and $P_2(t) = \bar{P}_2$ the equilibrium equations will be

$$\begin{cases} \bar{V}_{1e} = (\bar{P}_1 + \bar{P}_2 + c_5\bar{E}_1 + c_4\bar{E}_2)H_{1e}(0) - c_2\bar{I}H_i(0) \\ \bar{V}_{2e} = c_3\bar{E}_1 H_{1e}(0) \\ \bar{V}_i = c_1\bar{E}_1 H_{1e}(0), \end{cases} \qquad (3.1.1)$$

$$\begin{cases} \bar{E}_1 = \lambda_e g(\bar{V}_{1e}) \\ \bar{E}_2 = \lambda_e g(\bar{V}_{2e}) \\ \bar{I} = \lambda_i g(\bar{V}_i). \end{cases} \qquad (3.1.2)$$

There is always at least one solution to these equations but there may be several, in fact three solutions for the assumed nonlinearity (2.3.6). This is interesting since it indicates the possibility for the system to jump between two stable operating points. However for the case $c_1 = c_3$, c_5 fairly small, and $c_2\lambda_i$

$> c_4 \lambda_e$ there is only one solution. These conditions will make the negative feedback loop to dominate at all input levels. The conclusion is valid in general that with a dominating negative feedback loop there is only one steady state solution.

3.2. Linearized Equations and Stability

With the steady state values subtracted from the system variables the result will be new variables denoted $v_{1e}(t)$, $v_{2e}(t)$, $v_i(t)$, $e_1(t)$, $e_2(t)$, and $i(t)$. The corresponding Laplace transforms are denoted $V_{1e}(s)$, $V_{2e}(s)$, $V_i(s)$, $E_1(s)$, $E_2(s)$, and $I(s)$. Next the nonlinearities are linearized around the operating points defined by (3.1.1) and (3.1.2).

$$\begin{cases} e_1(t) \approx d_{1e} v_{1e}(t) \\ e_2(t) \approx d_{2e} v_{2e}(t) \\ i(t) \approx d_i v_i(t). \end{cases} \tag{3.2.1}$$

Similar relations hold for the Laplace transformed variables.

$$\begin{cases} E_1(s) = d_{1e} V_{1e}(s) \\ E_2(s) = d_{2e} V_{2e}(s) \\ I(s) = d_i V_i(s). \end{cases} \tag{3.2.2}$$

This last set of equations together with the following set define equilibrium equations

$$\begin{cases} V_{1e}(s) = (P_1(s) + c_5 E_1(s)) H_{1e}(s) \\ \qquad + (P_2(s) + c_4 E_2(s)) H_{2e}(s) - c_2 I(s) H_i(s) \\ V_{2e}(s) = c_3 E_1(s) H_{1e}(s) \\ V_i(s) = c_1 E_1(s) H_{1e}(s). \end{cases} \tag{3.2.3}$$

When these equations are solved for $E_1(s)$ the result will be

$$E_1(s) = \frac{d_{1e} H_{1e}(s)}{N(s)} P_1(s) + \frac{d_{1e} H_{2e}(s)}{N(s)} P_2(s) \tag{3.2.4}$$

with

$$N(s) = 1 - D_{ee} H_{1e}(s) H_{2e}(s) - D_e H_{1e}(s) \\ + D_{ei} H_{1e}(s) H_i(s) \tag{3.2.5}$$

. and

$$\begin{cases} D_{ee} = c_3 c_4 d_{1e} d_{2e} \\ D_e = c_5 d_{1e} \\ D_{ei} = c_1 c_2 d_{1e} d_i. \end{cases} \tag{3.2.6}$$

These last constants serve as coupling coefficients for the feedback loops.

Expressions $d_{1e} H_{1e}(s)/N(s)$ and $d_{1e} H_{2e}(s)/N(s)$ define transfer functions between the input variables and the output $E_1(s)$. They differ only through the delay factor in (2.3.4).

It is now of interest to find out when the linearized system is stable which requires that the poles of $H_{1e}(s)/N(s)$ are located in the left half of the s-plane. Only the case $\tau_d = 0$ is considered, i.e. $H_{2e}(s) = H_{1e}(s)$, which will make $H_{1e}(s)/N(s)$ a rational function with a denominator of fifth degree. A Hurwitz stability test has been applied which imposes restrictions on the coupling coefficients. Results are shown in Fig. 2 for different system configurations where input level $\bar{P} = \bar{P}_1 + \bar{P}_2$ and parameter c_2 have been selected as variables. For each combination of these the values of the coupling coefficients are shown and the region of stability is indicated. Figure 2a applies for the case of only a negative feedback loop and hence values of D_{ei} are shown. Figure 2b describes the situation with the negative feedback loop and the positive loop defined by c_5. In this case values of D_{ei} and D_e are shown. Figure 2c, finally, covers the case with the negative loop and the positive loop defined by c_3 and c_4. To simplify the analysis $c_3 = c_1$ which implies that the configuration can be reduced to contain only two nonlinearities.

The stability region has about the same shape for all three configurations. When the input level is increased from a low value it will drive the system into instability except when c_2 is small. A further increase of $\bar{P}$ will make the system pass the instability region and once more become stable. This is natural since low and high input levels will cause the system to operate with low amplification around the feedback loops while intermediate values will make it operate in the steep part of the nonlinearities which may cause instabilities. An interesting observation can be made from the diagrams, namely that a decrease of c_2 may drive the system from stability into instability if the input level is sufficiently large.

3.3. The Transfer Function

With the system in stable condition it will function essentially as a linear filter for small variations of the input signal. It is of special interest to apply a signal of white noise added to $\bar{P}$ which will serve as a model of variations in the pulse intensity from receptor neurons. In this case the system will shape the spectrum of the output signal. To study the situation we have calculated the absolute value of the transfer function $d_{1e}|H_{1e}(j\omega)/N(j\omega)|$ for various sets of parameters.

Figure 3a shows a set of curves that apply for the system with only the negative feedback loop connected. An increase of $\bar{P}$ will shift the peak frequency to higher values and sharpen the peak. The shape is determined by D_{ei} only and Fig. 2a can be used to find the locus for identical transfer functions. The scale of the abscissa has been normalized in the most con-
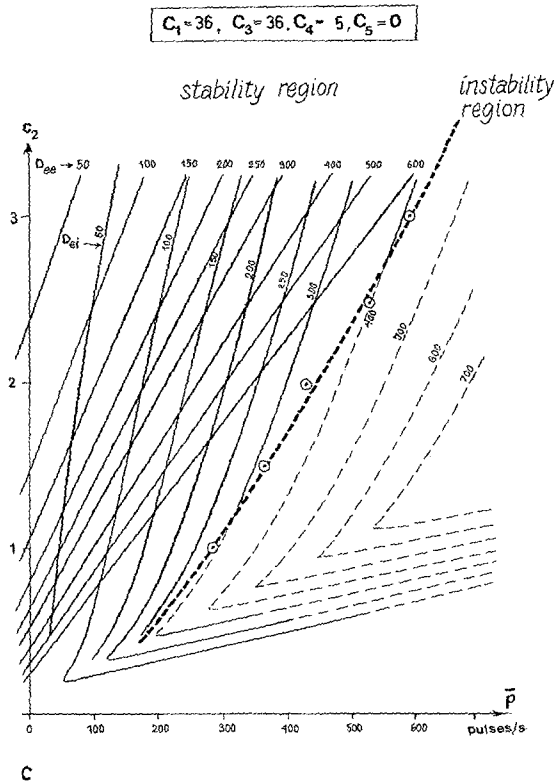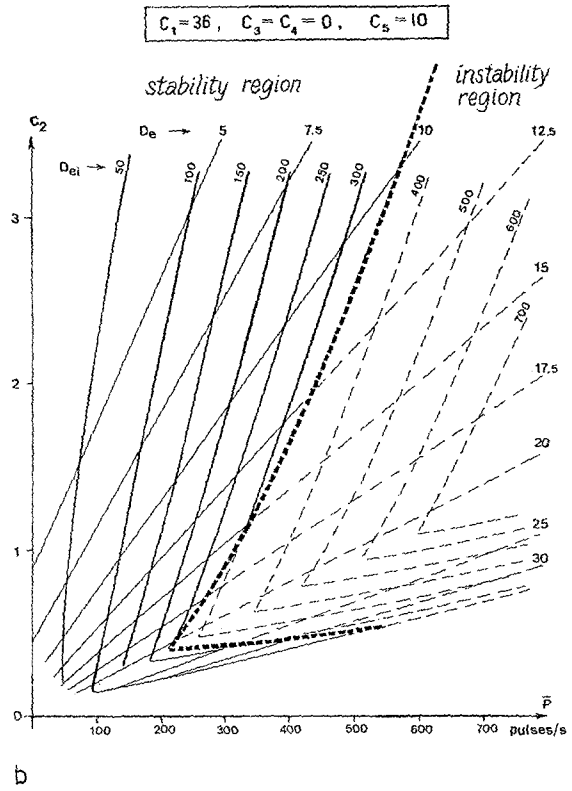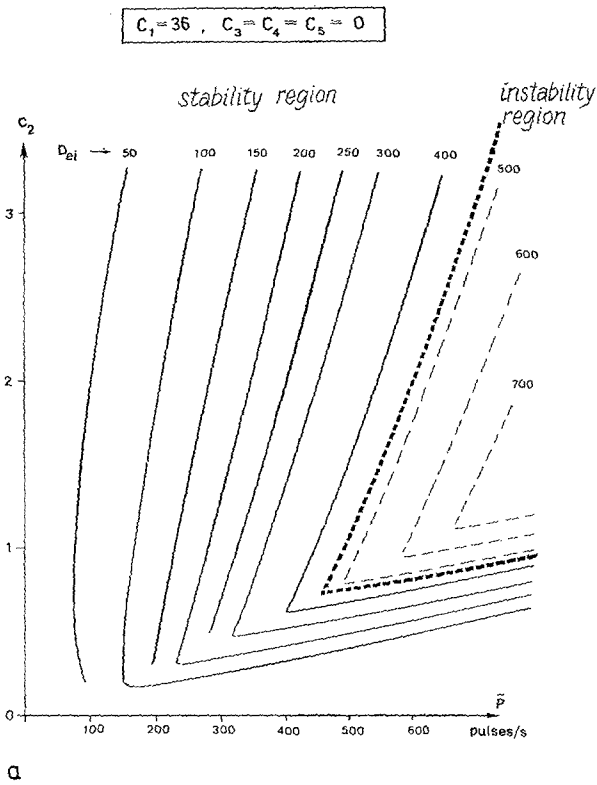
a

b

c

Fig. 2a–c. Stability diagrams for system in Fig. 1b with a negative feedback loop only, b negative and linear positive feedback loops c negative and positive nonlinear feedback loops

venient way by the programmer. Actually the absolute amplitude will increase strongly with an increase of $\bar{P}$. The diagram is intended to show only changes in the shape.

Calculations have been done with either one of the positive feedback loops included in addition to the negative one and similar changes in shape were observed for increasing values of $\bar{P}$ (Zetterberg et al., 1977).

A set of curves in Fig. 3b shows how the extra delay τ_d defined in (2.3.4) will affect the performance when the network has a positive feedback loop through c_3 and c_4 while $c_5 = 0$. The result of increasing τ_d in the range 0 to 30 ms is a decrease in peak amplitude and only a small change in peak frequency. Other calculations show that for large delays the peak frequency is also changed.

4. Limit Cycle Analysis

4.1. General Relations

Previously it was found that the network will become unstable for certain parameter values and input levels $\bar{P}$. The behaviour of the system under these conditions will be investigated in this section by means of describing functions technique, see for example Šiljak (1969). It is then assumed that periodic oscillations will appear in the network such that the signal at the input to a nonlinearity is essentially sinusiodal. The nonli-

21

nearities will produce harmonics but these will be attenuated in the filters following the nonlinearities. It is then essential that the filters are of low pass type which is the case for the actual system.

The configuration of primary interest is the one with only the negative feedback loop present. The more general case with a positive feedback loop also connected can be treated fairly easily for the case $c_3 = c_1$ which makes the system equivalent to that with one feedback loop only if the filters are appropriately changed. The case with $c_3 = c_4 = 0$ but $c_5 > 0$ can also be handled fairly easily. In all cases the system will include two nonlinearities of the same functional form written $g(v)$ according to (2.3.6).

Let the input to one of the nonlinearities be denoted

$$u(t) = u_0 + u_1 \cos(\omega t + \varphi). \tag{4.1.1}$$

After passing the nonlinearity the signal may be written

$$y(t) = y_0 + y_1 \cos(\omega t + \varphi) + y_2 \cos(2\omega t + 2\varphi) + \dots . \tag{4.1.2}$$

The coefficients in this Fourier series are functions of u_0 and u_1 which may be expressed explicitly

$$y_0(u_0, u_1) = \frac{1}{\pi} \int_0^\pi g(u_0 + u_1 \cos x) dx, \tag{4.1.3}$$

$$y_n(u_0, u_1) = \frac{2}{\pi} \int_0^\pi g(u_0 + u_1 \cos x) \cos nx \, dx. \tag{4.1.4}$$

Numerical integration of (4.1.3) and (4.1.4) have been used to establish the diagrams in the following.

4.2. Network with only a Negative Feedback Loop

The assumption is that $c_3 = c_4 = c_5 = 0$ and for this case the equilibrium equations will be established for the steady state component and the first harmonic. For notations see Fig. 1b. Let

$$v_{1e}(t) = v_{10} + v_{11} \cos(\omega t + \varphi), \tag{4.2.1}$$

$$e_1(t) = e_{10} + e_{11} \cos(\omega t + \varphi), \tag{4.2.2}$$

with

$$e_{10} = \lambda_e y_0(v_{10}, v_{11}) ; \quad e_{11} = \lambda_e y_1(v_{10}, v_{11}). \tag{4.2.3}$$

From $e_1(t)$ the function $v_i(t)$ is found by a linear filter operation

$$v_i(t) = v_{i0} + v_{i1} \cos(\omega t + \varphi + \psi_{1e})$$
$$= e_{10} c_1 H_{1e}(0)$$
$$\quad + e_{11} c_1 |H_{1e}(j\omega)| \cos(\omega t + \varphi + \psi_{1e}), \tag{4.2.4}$$
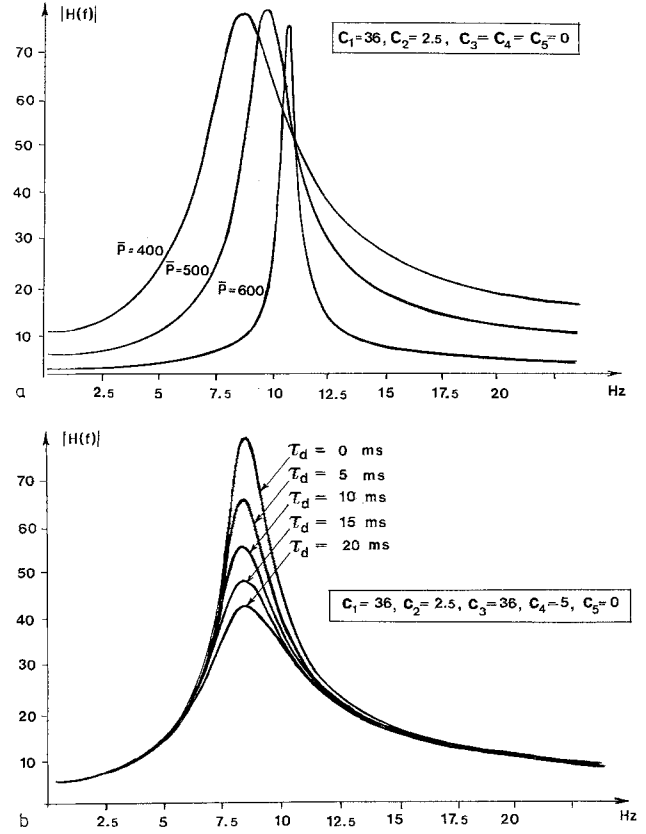

Fig. 3a and b. a Plot of normalized transfer function for system with negative feedback loop only with input level $\bar{P}$ as parameter, b plot of transfer function for system with negative and nonlinear positive feedback loops with delay parameter τ_d as parameter

with $\psi_{1e} = \arg H_{1e}(j\omega)$. Next the expression for $i(t)$ will be stated

$$i(t) = i_0 + i_1 \cos(\omega t + \varphi + \psi_{1e}) \tag{4.2.5}$$

with

$$i_0 = \lambda_i y_0(e_{10} c_1 H_{1e}(0), e_{11} c_1 |H_{1e}(j\omega)|), \tag{4.2.6}$$

$$i_1 = \lambda_i y_1(e_{10} c_1 H_{1e}(0), e_{11} c_1 |H_{1e}(j\omega)|). \tag{4.2.7}$$

After another filter operation through $h_i(\tau)$ the result will be

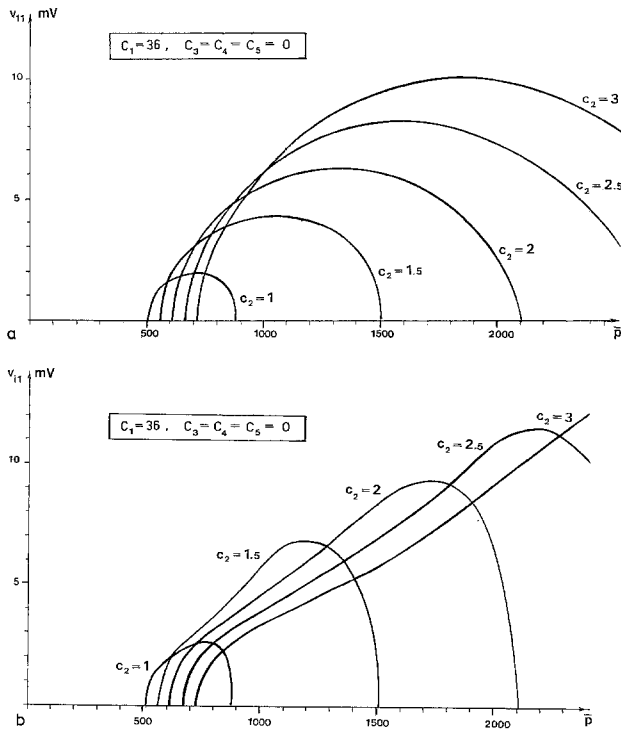$$i_0 c_2 H_i(0) + i_1 c_2 |H_i(j\omega)| \cos(\omega t + \varphi + \psi_{1e} + \psi_i). \tag{4.2.8}$$

The equilibrium equations may now be written

$$\begin{cases} v_{10} = \bar{P} H_{1e}(0) - i_0 c_2 H_i(0), \\ v_{11} = -i_1 c_2 |H_i(j\omega)| \cos(\psi_{1e} + \psi_i), \\ 0 = \sin(\psi_{1e} + \psi_i). \end{cases} \tag{4.2.9}$$

The last two equations will require $\psi_{1e} + \psi_i = (2m + 1)\pi$ for some integers m and hence

$$\tan \psi_{1e} = -\tan \psi_i. \tag{4.2.10}$$

With these functions calculated from (2.3.3) the result

Fig. 4a and b. Limit cycle analysis of system with negative feedback loop only **a** amplitude of first harmonic v_{11} for excitatory subset, **b** amplitude of first harmonic v_{i1} for inhibitory subset

will be a relation that determines $\omega = \omega_0$

$$\omega_0^2 = \frac{a_i b_i(a_e + b_e) + a_e b_e(a_i + b_i)}{a_e + b_e + a_i + b_i}. \tag{4.2.11}$$

The formula will give $f_0 = 11.3\,\text{Hz}$.

Hence for the configuration considered the period of the oscillations is determined by the EPSP and IPSP filters only. The amplitudes may be found from the first two equations (4.2.9)

$$\begin{cases} v_{10} = \bar{P} H_{1e}(0) - i_0 c_2 H_i(0), \\ v_{11} = i_1 c_2 |H_i(j\omega_0)|. \end{cases} \tag{4.2.12}$$

Variables i_0 and i_1 are expressed in terms of v_{10} and v_{11}, through (4.2.6), (4.2.7), and (4.2.3).

Numerical results are shown in Fig. 4a and b for v_{11} and v_{i1} respectively as a function of $\bar{P}$ with c_2 as a parameter. Oscillations occur within a certain range of $\bar{P}$ which coincides with values found in Fig. 2a. As soon as oscillations start v_{10} and v_{i1} will be changed and hence the operating point for the two non-linearities but, the changes are small for small amplitudes v_{11} and v_{i1}.

4.3. Network with a Negative and a Positive Feedback Loop

Only the case with a positive feedback loop through the nonlinear loop defined by c_3 and c_4 is considered

for $c_3 = c_1$. The analysis in the last section will apply when $c_2 H_i(s)$ is replaced by $c_2 H_i(s) - c_4 H_{2e}(s)$. Also this time the resonance frequency is determined solely by the filters involved. Results are found in Zetterberg et al. (1977) for the case $c_1 = c_3 = 36$, $c_4 = 5$ and several values of c_2. In all cases $\tau_d = 0$, i.e. $H_{2e}(s) = H_{1e}(s)$. Qualitatively results are similar to those in the last section but amplitudes are larger and oscillations occur for smaller values of $\bar{P}$.

5. Electronic Circuit Model

5.1. Circuit

An electronic circuit has been built based on the block diagram of Fig. 1b. The linear filters are realized as simple active RC-circuits, Zetterberg et al. (1977), with no extra delays, τ_d, involved and hence $h_{2e}(\tau) = h_{1e}(\tau)$. DC voltages are applied to attain the appropriate operating points. The nonlinearities are constructed with diodes and the result is a nonlinear function that closely resembles $g(v)$ of (2.3.6) with $\gamma = 0.34$ and $v_0 = 6\,\text{mV}$. In the circuit the coefficients c_1, c_2, c_3, and c_4 may be adjusted by means of potentiometers while $c_5 = 0$.

5.2. Measurements

First the network is studied under stable conditions with white noise as input. The situation will resemble that analyzed in Sect. 3 but nonlinear effects will be taken into account. Figure 5 show recorded signals and analyzed spectral densities for the network with only the negative feedback loop connected. The diagrams refer to three different input levels, $V_{in} = 5, 7$, and $10\,\text{V}$ corresponding to $\bar{P} = 180$, 260, and 360. The spectral plots are calculated with a Kalman filter program for model order $p = 7$ and $q = 6$ and time increment 1.6 s between successive curves (Isaksson, 1977). A similar set of curves applies to the network with both a positive and a negative feedback loop for which $c_1 = 36$, $c_2 = 2.5$, $c_3 = 36$, and $c_4 = 5$, Zetterberg et al. (1977). In both sets of curves there is a shift of the main resonance frequency to higher values and more stable waves as $\bar{P}$ increases. This is in accordance with results from Sect. 3.3. It is noticed that the network produces activity also at low frequencies, δ-activity, which becomes stronger as $\bar{P}$ increases. There is also contributions, from higher frequencies around the second harmonic of the main resonance frequency. This is produced by the nonlinearity and it may be one plausible mechanism for the generation of β-activity. The spectral analysis indicates considerable variations in parameters for each analyzed segment and hence the processes are not particularly stationary.
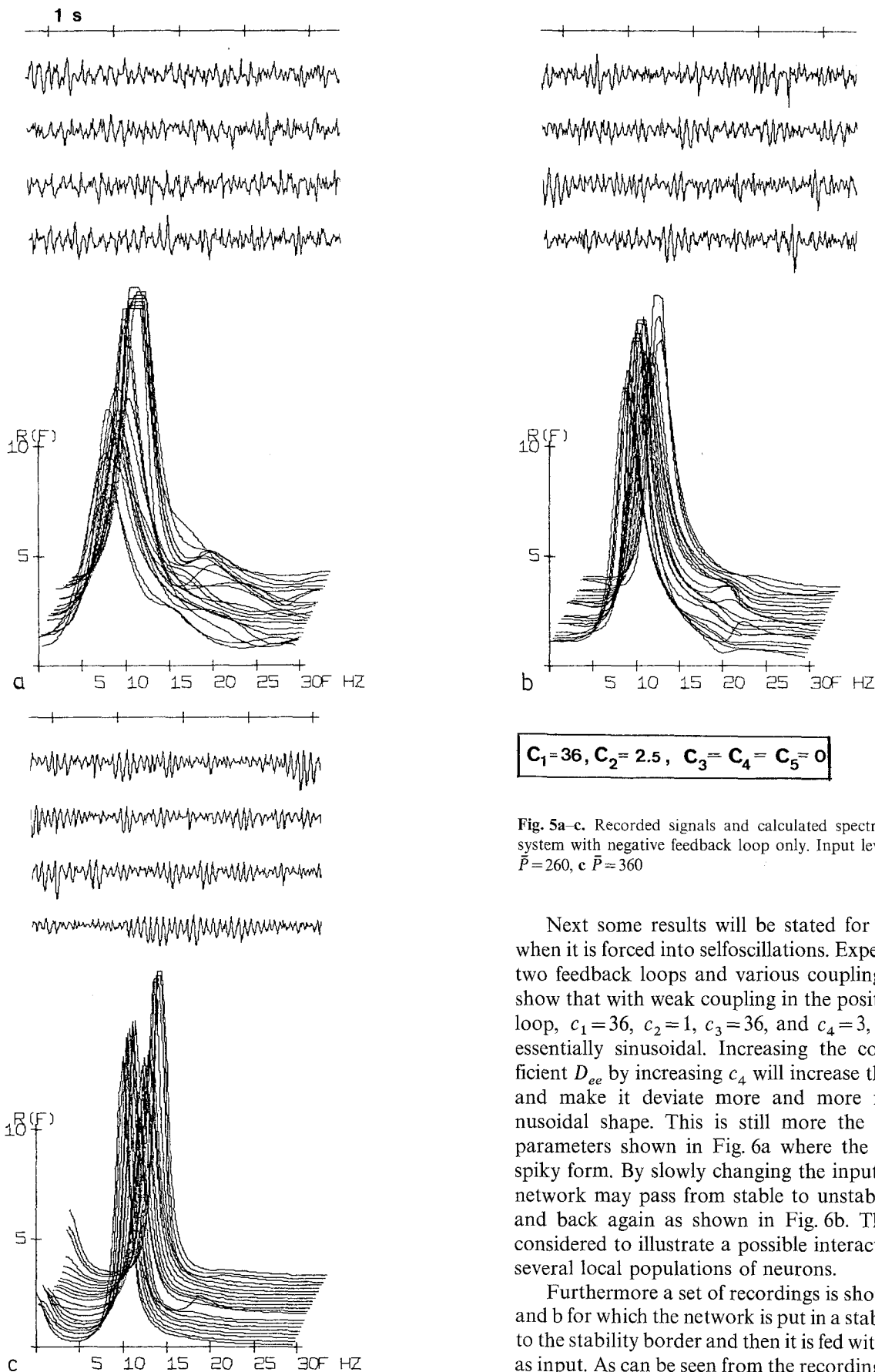
1 s

$C_1 = 36, C_2 = 2.5, C_3 = C_4 = C_5 = 0$

Fig. 5a–c. Recorded signals and calculated spectra for electronic system with negative feedback loop only. Input levels **a** $\bar{P} = 180$, **b** $\bar{P} = 260$, **c** $\bar{P} = 360$

Next some results will be stated for the network when it is forced into selfoscillations. Experiments with two feedback loops and various coupling coefficients show that with weak coupling in the positive feedback loop, $c_1 = 36$, $c_2 = 1$, $c_3 = 36$, and $c_4 = 3$, the signal is essentially sinusoidal. Increasing the coupling coefficient D_{ee} by increasing c_4 will increase the amplitude and make it deviate more and more from the sinusoidal shape. This is still more the case for the parameters shown in Fig. 6a where the signal has a spiky form. By slowly changing the input level V_0 the network may pass from stable to unstable behaviour and back again as shown in Fig. 6b. This case was considered to illustrate a possible interaction between several local populations of neurons.

Furthermore a set of recordings is shown in Fig. 7a and b for which the network is put in a stable state close to the stability border and then it is fed with white noise as input. As can be seen from the recordings occasional
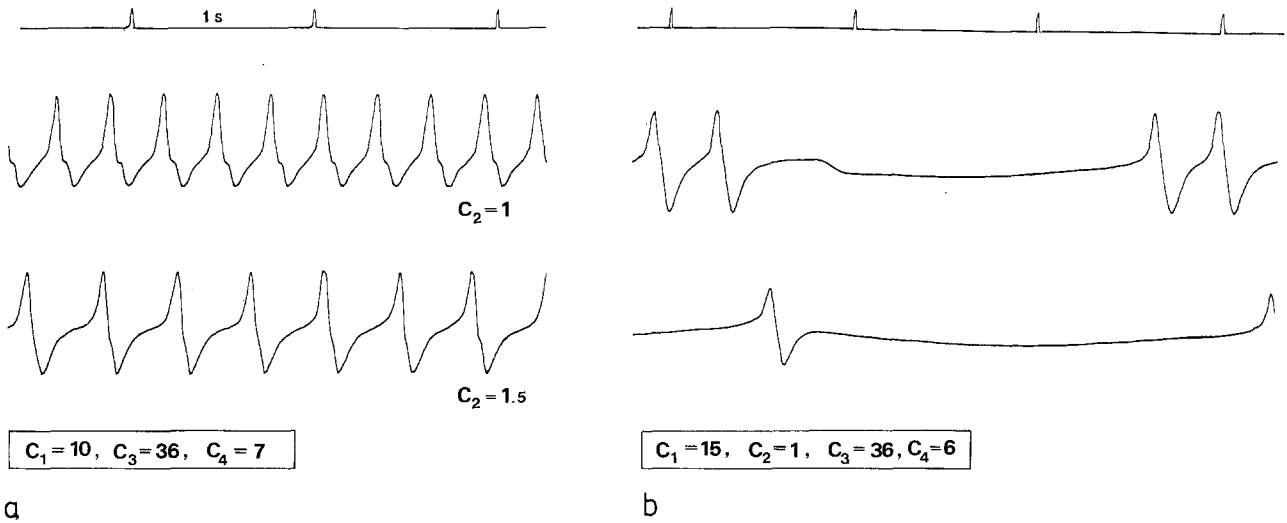
Fig. 6a and b. Recorded signals during limit cycle behavior for electronic system with negative and positive feedback loops **a** fixed input level $\bar{P}$ **b** slowly varying input level $\bar{P}$
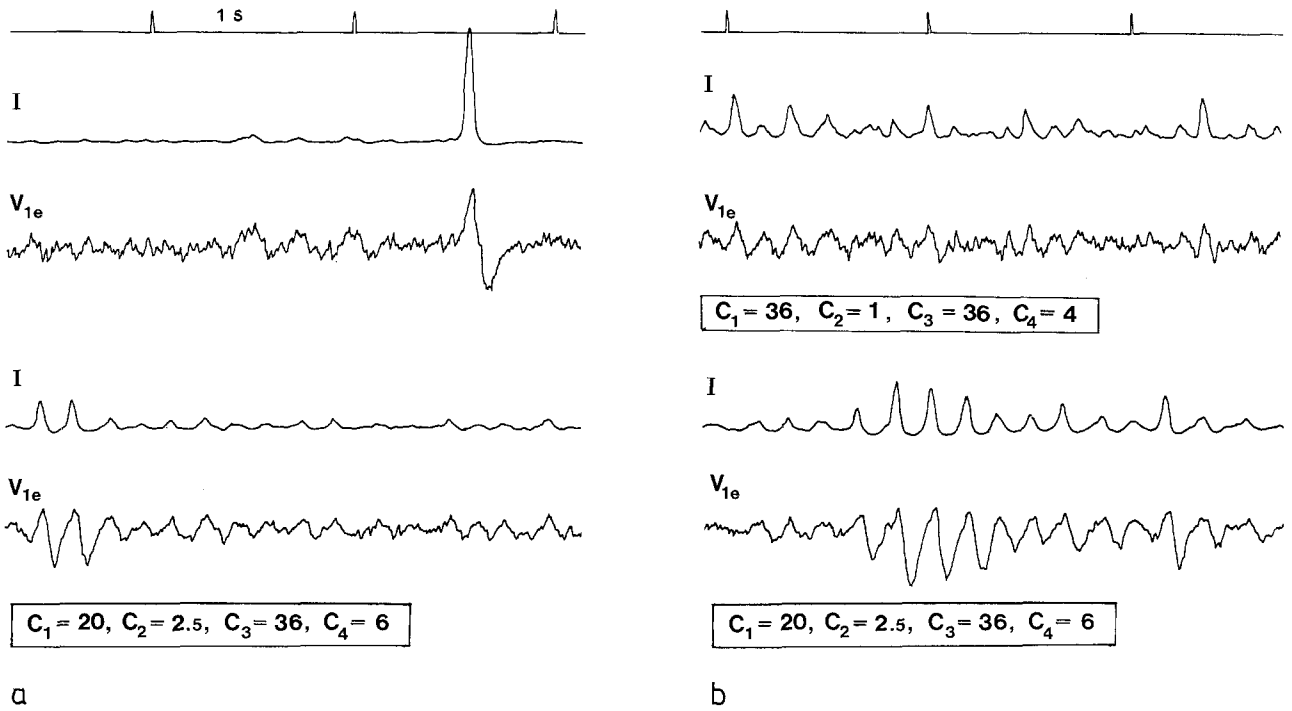

Fig. 7a and b. Recorded signals during limit cycle behavior for electronic system with negative and positive feedback loops. Input $\bar{P}$ fixed level plus white noise **a** fixed level 180 **b** fixed level 90 and 180

instabilities occur which may produce spikes or sustained oscillations depending on the conditions.

Based on these and many other recordings it may be concluded that the electronic network may be used to produce signals that resemble those recorded from the brain. With the network operating in stable conditions with white noise as input the result is similar to normal background EEG activity. With the network in unstable condition the waveforms are alike some of those produced in epileptic states. To illustrate this more specifically, Fig. 8a has been reproduced which shows a recording from the rabbit brain made at the Neurophysiological Institute in Vienna, see also Petsche and Šterc (1968). The uncovered cortex is electrically stimulated and the result is periodically interrupted oscillations. We have tried to imitate that
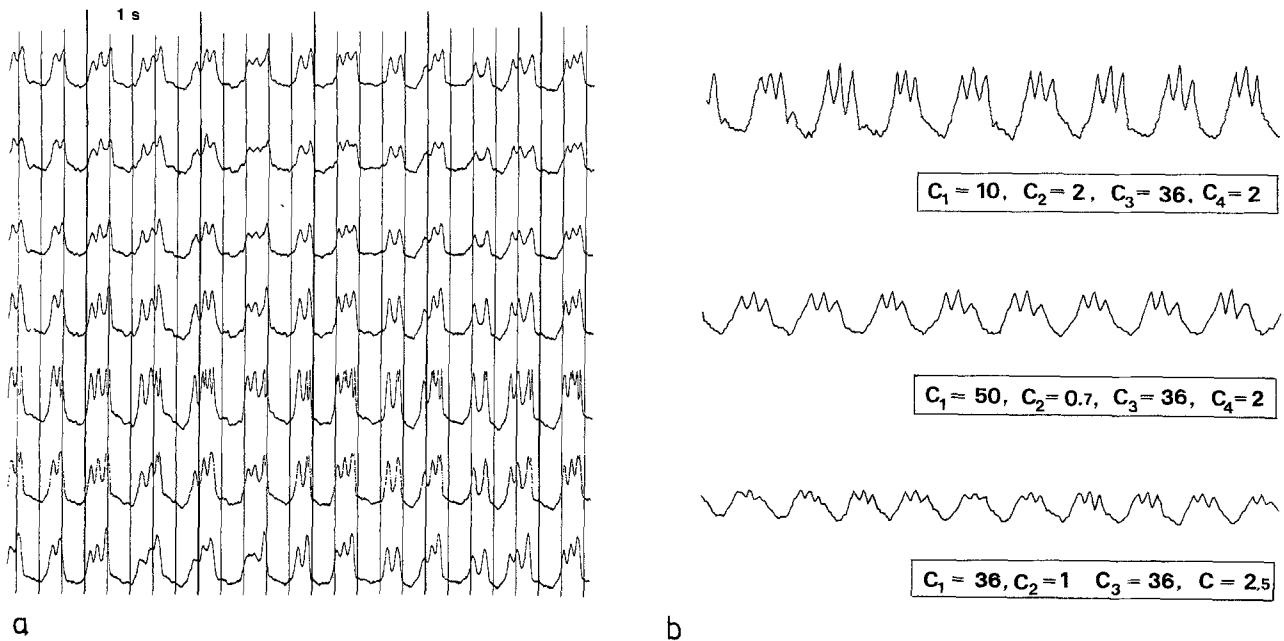
Fig. 8a and b. a Recordings from uncovered rabbit cortex stimulated by electrical signals, **b** simulations on electronic model with input signal sinusoidal plus white noise

signal by driving the network with an external sinusoidal signal of high amplitude which forces the network into oscillations for part of the period, see Fig. 8b. The recordings have a fair similarity. Similar results have been achieved by stimulating the rabbit brain with penicillin. However it has not been possible to reproduce all wave forms that appear in these created epileptic situations.

Comments

The model as formulated in Fig. 1b is shown to produce signals that resemble background EEG activity. This means that the linear analysis should apply fairly well. The model is less accurate for describing seizure activity as expressed in the occurence of limit cycles. This is due to the approximations involved in going from (2.1.4) and (2.1.5) to (2.1.6) and (2.1.7). However the condition under which limit cycles occur should still be relevant and the main characteristics of limit cycles as shown in Fig. 4 should still hold true. A recent paper by Kaczmarek and Babloyantz (1977) gives further insight into the mechanism of seizure activity.

Experiments performed with our model has brought up the hypothesis that epileptic spikes are generated in a population of neurons that operate close to instability. If this is true spikes may be viewed as borderlike cases between normal background activity and seizure activity.

References

Creutzfeld (ed.): Electrical activity from the neuron to the EEG and EMG; Part C: The neuronal generation of the EEG. In: Handbook of electroencephalography and clinical neurophysiologi. Amsterdam: Elsevier 1974

Etevenon, P., Levy, J.C.: Simulation sur ordinateur d'electroencephalogrammes normaux et pathologiques. Congres d'Informatique Médicale de l'IRIA, Tome I, 265–281, Toulouse, 1973

Freeman, W.J.: Linear analysis of the dynamics of neural masses. Ann. Rev. Biophys. Bioeng. **1**, 225–256 (1972)

Freeman, W.J.: Mass action in the nervous system. New York: Academic Press 1975

Isaksson, A.: SPARK – A sparsely updated Kalman filter with application to EEG signals. Tech. Rep. No. 120. Telecommunication Theory, Royal Inst. of Techn., Stockholm (1973)

Isaksson, A., Wennberg, H.: An EEG simulator – A means of objective clinical interpretation of EEG. Electroenceph. clin. Neurophys. **39**, 313–320 (1975)

Kaczmarek, L.K., Babloyantz, A.: Spatiotemporal pattern in epileptic seizures. Biol. Cybernetics **26**, 199–208 (1977)

Levy, J.C., Etevenon, P.: Un modèle d'électroencéphalogramme comparé aux tracés veille-sommeil du rat. Psych. Méd. (Paris) **4**, 695–701 (1972)

Lopes da Silva, F.H., Barts, P., van Heuschen, E., van Rotterdam, A., Burr, W.: Models of neuronal populations, the basic mechanism of rhythmicity. In: Perspectives in Brain Research Ser. Progress in Brain Research. Amsterdam: Elsevier 1976

Lopes da Silva, F.H., Hoeks, A., Smits, H., Zetterberg, L.H.: Model of brain rhythmic activity, the alpha-rhythm of the thalamus. Kybernetik **15**, 27–37 (1974)

Petsche, H., Šterc, J.: The significance of the cortex for the travelling phenomenon of brain waves. Electroenceph. clin. Neurophysiol. **25**, 11–22, (1968)

26

Šiljak, D.D.: Nonlinear systems. New York: Wiley 1969

Stevens, C.F.: Neurophysiology: a primer. New York: Wiley 1966

Wilson, H.R., Cowan, J.D.: Excitatory and inhibitory interaction in localized populations of model neurons. Biophys. J. **12**, 1–23 (1972)

Wilson, H.R., Cowan, J.D.: A mathematical theory of the functional dynamics of cortical and thalamic nervous tissue. Kybernetik **13**, 55–80 (1973)

Zetterberg, L.H.: Stochastic activity in a population of neurons – a system analysis approach. Report Inst. Med. Physics TNO, Utrecht **1**, 153 (1973)

Zetterberg, L.H., Kristiansson, L., Mossberg, K.: Analysis and experiments with a model of a local neuron population. Technical Report No. 125, Telecommunication Theory, Royal Inst. of Techn. Stockholm, 1977

Dr. Lars H. Zetterberg
Dept. for Telecommunication Theory
Royal Inst. of Technology
S-10044 Stockholm
Sweden